

Published in final edited form as:

Respir Physiol Neurobiol. 2009 October 31; 169(1): 44–49. doi:10.1016/j.resp.2009.07.024.

Marked pericardial inhomogeneity of specific ventilation at total lung capacity and beyond

Yanping Sun^{1,6}, James P. Butler², Peter Lindholm³, Ronn Walvick⁶, Stephen H. Loring⁴, Jessica Gereige¹, Massimo Ferrigno⁵, and Mitchell S. Albert^{1,6,*}

¹Department of Radiology, Brigham and Women's Hospital, Harvard Medical School, Boston, Massachusetts 02115; Mitchell.albert@umassmed.edu; yanping.sun@umassmed.edu

²Molecular and Integrative Physiological Science Program, Department of Environmental Health, Harvard School of Public Health, and Department of Medicine, Harvard Medical School, Boston, MA 02115; JBUTLER@hsph.harvard.edu

³Department of Radiology, Karolinska Hospital and Department of Physiology and Pharmacology Karolinska Institutet, Stockholm, 17177, Sweden; Peter.Lindholm@ki.se

⁴Department of Anesthesia, Critical Care and Pain Medicine, Beth Israel Deaconess Medical Center, Harvard Medical School, Boston, MA 02215; sloring@bidmc.harvard.edu

⁵Department of Anesthesiology, Perioperative and Pain Medicine, Brigham and Women's Hospital, Harvard Medical School, Boston, MA 02115; MFERRIGNO1@PARTNERS.ORG

⁶Department of Radiology, University of Massachusetts Medical School, Worcester, MA 01655; Mitchell.albert@umassmed.edu; yanping.sun@umassmed.edu

Abstract

We measured regional ventilation at 1 liter above functional residual capacity (FRC+1L) and total lung capacity (TLC) in three normal subjects and four elite breath-hold divers, and above TLC after glossopharyngeal insufflation (TLC+GI) in the divers. Hyperpolarized ³He MRI was used to map the local ventilation per unit volume over the entire lung. At TLC and above, there was markedly increased regional ventilation of the lungs in the pericardial region compared with the relatively uniform ventilation throughout the rest of the lung. The distribution of fractional ventilation regionally was relatively uniform at FRC+1L, with a small non-gravitational cephalocaudal gradient of specific ventilation in the supine posture. Our observations at high lung volumes are consistent with the effect of high pleural tension in the concave pericardial region, which promotes expansion of the subjacent lung, leading to a higher local effective compliance and a higher specific ventilation.

Keywords

hyperpolarized helium MRI; glossopharyngeal breathing; glossopharyngeal insufflation; breath-hold diver; lung volumes

© 2009 Elsevier B.V. All rights reserved.

*Corresponding author: Mitchell Albert, Ph.D., Department of Radiology, University of Massachusetts Medical School, 55 Lake Avenue North, Worcester, MA 01655, Tel: 508-856-1096, Fax: 508-856-6250, mitchell.albert@umassmed.edu

Publisher's Disclaimer: This is a PDF file of an unedited manuscript that has been accepted for publication. As a service to our customers we are providing this early version of the manuscript. The manuscript will undergo copyediting, typesetting, and review of the resulting proof before it is published in its final citable form. Please note that during the production process errors may be discovered which could affect the content, and all legal disclaimers that apply to the journal pertain.

1. Introduction

It is widely believed that near total lung capacity (TLC), i.e., the maximal lung volume that can be achieved voluntarily with an open glottis, expansion of the healthy mammalian lung is nearly completely homogeneous. This belief is traceable to two classical works. One study is structural in nature; Glazier et al. (1967) studied the distribution of alveolar size in frozen sections of dog lungs as a function of height within the lung. They found that at low and mid lung volumes the distribution of alveolar sizes was a strong function of height, the dependent alveoli being smaller, but at TLC, alveolar size was uniform. The other is a functional study in awake upright humans by Milic-Emili (1966) in which the regional distribution of inspired gas was measured as a function of vertical height over a range of lung volumes. The resulting graph, celebrated as “Milic’s onion”, shows the volume of various lung regions relative to volume at TLC at different heights plotted against total lung volume. By construction, all these curves converge to a point at TLC. For example, at low- to mid-lung volumes, the upper regions of the lung are filled to a greater volume but have a lower specific compliance, and therefore, a lower specific ventilation. Although these works imply the uniformity of lung *expansion* at TLC, they do not speak to the uniformity of *ventilation* at TLC. Indeed, Milic’s onion shows that the slopes of the regional volume/total volume curves differ at TLC, reflecting a regional variation in specific compliance with height. Studies of lung expansion using low resolution radioactive tracers usually showed relatively homogeneous expansion within an iso-gravitational region. Such gravitational variation in alveolar expansion (Milic-Emili, 1986) is the origin of the cephalocaudal gradient in distribution of tidal ventilation in the upright position (Engel, 1986). In the supine posture, there are small gradients in specific ventilation related to regional specific compliance and chest wall factors (Engel, 1986).

We recently conducted physiologic studies of elite breath-hold divers (Loring, 2007), who are able to increase their lung volumes significantly above TLC using a peculiar glossopharyngeal maneuver, commonly called “lung packing” in the diving community (Lindholm, 2005; Seccombe, 2006), here referred to as glossopharyngeal insufflation (GI). This maneuver, in which boluses of air are repeatedly pushed into the lungs by rhythmic contractions of the glossopharyngeal muscles, was developed in the 1950’s by patients with weak or dysfunctional respiratory muscles to increase their lung volumes and to improve cough (Dail, 1951). During GI, air is taken into the mouth and pharynx that then contracts in a coordinated sequence; this includes elevation of the larynx, opening of the glottis and posterior displacement of the tongue, as air is injected into the trachea. As the next intake of air occurs, the larynx drops down with closed vocal cords, pushing the entrapped air into the lungs. This maneuver is usually repeated a few times. For a detailed description, see Lindholm et al. (2009).

In the subsequent years, with the decline in the number of polio patients, the clinical use of GI has become less frequent, but is still practiced by some patients. Meanwhile GI maneuvers have been adopted by breath-hold divers, allowing them to prolong their dives by increasing oxygen stores in the lungs and to reach greater depths by starting their dives with larger lung volumes. Recently, the clinical use of GI has again been proposed in the field of rehabilitation medicine (Nygren-Bonnier, 2008).

We hypothesized that whereas both normal subjects and elite divers show relatively uniform or smoothly varying specific ventilation at TLC, there could be significant deviations from uniformity in the divers at volumes above TLC. We therefore undertook a series of experiments measuring regional ventilation at various lung volumes, including FRC+1L, TLC, and after GI (TLC+GI). To do this, we utilized recent developments in the use of hyperpolarized ^3He and magnetic resonance imaging (MRI) techniques to map quantitatively the local ventilation per unit volume over the entire lung. Importantly, this technology provides comparable spatial resolution to radioactive tracer techniques but does not involve ionizing radiation as in

ventilation scintigraphy with ^{133}Xe (Altes, 2004) or computerized tomography (Brenner, 2007), thus allowing multiple experiments in the same subjects.

2. Materials and Methods

2.1 SUBJECTS

Seven subjects, 3 females and 4 males, aged 21-32 y, were studied. Heights ranged from 1.60 to 1.85 m, and weights from 54 to 80 kg. All of the subjects were rather slim and none was obese. Three of the males and one female subject were elite breath-hold divers used to performing GI maneuvers. Data from spirometry and pulmonary pressures in these divers during GI have been published (Loring, 2007). The other male and two females were normal subjects; all subjects were healthy non-smokers.

The protocol was approved by the Human Research Committee at Brigham and Women's Hospital. Written informed consent was obtained from all subjects. All experiments were carried out with a pulmonary physician present.

2.2 MRI ACQUISITION

MR imaging was carried out on a General Electric Signa LX 1.5T MRI scanner. For MRI using hyperpolarized ^3He , a heterodyne system was appended to the MRI system to enable imaging at the ^3He Larmor frequency. The signal was collected using a flexible quadrature wrap-around lung coil (Clinical MR Solutions, Brookfield, WI) tuned to the ^3He frequency.

^3He was hyperpolarized via collision spin exchange with optically-pumped rubidium (Happer, 1984) using a locally made ^3He polarizer, achieving polarizations between 10 and 20%. The scans employed a Fast Gradient Echo pulse sequence acquiring coronal multi-slice images with the following parameters: 46 cm FOV (Field of View), 0.75 PhaseFOV, 128×256 matrix, 13 mm slice thickness, 0 mm gap between slices, 31.25 kHz bandwidth, 14°-18° flip angle, TE/TR (Echo Time/ Repetition Time) 1.228 ms/50-75 ms, and interleaved data acquisition. Scans ranged from 5-10 seconds, depending on the anterior-posterior depth of the lungs, which may require 9 to 14 slices to encompass. The acquired data were then zero-padded to produce images with 256×256 pixels.

Two vital capacity maneuvers were done to standardize lung volume history prior to ventilation scans. Ventilation scans were performed with subjects in the supine position. During these scans, subjects were instructed to inhale a $^3\text{He}/\text{N}_2$ gas mixture (consisting of 330ml of hyperpolarized ^3He , and 670ml of nitrogen) from a 1-liter Tedlar bag over an inspiratory time of a few seconds, and then hold their breath. Specifics of the maneuvers are described below. Scanning began immediately upon breath hold. After completion of the scan, the subject was instructed to breathe normally.

2.3 MANEUVERS

Subjects performed ^3He inhalation maneuvers at FRC+1L, and TLC; the divers performed an additional maneuver, inhaling ^3He during glossopharyngeal insufflation, to TLC+GI. The GI maneuver itself was accomplished in 10-15 s. Specific protocols at target volumes (FRC+1L) (n=5, 2 divers, 3 normals). The subjects were instructed to take in a normal inspiration, followed by a normal expiration. This leaves the lungs at functional residual capacity. The subject then inhaled the 1-liter ^3He gas mixture and held his/her breath during the scan.

TLC (n=7, all subjects) The subjects first inhaled air to total lung capacity, they then exhaled 1 liter of air into an empty 1L Tedlar bag, and subsequently inhaled the 1 liter of ^3He gas mixture from an identical Tedlar bag and held their breath while the scanning was in progress.

TLC+GI (n=4, divers) The subjects first inhaled air to total lung capacity and performed the glossopharyngeal insufflation maneuver repeatedly to a volume where they would still be able to insufflate another liter of gas (as learned through sham trials). Then they insufflated the liter of the ^3He gas mixture from the Tedlar bag and held their breath while the scanning was in progress. For two of the divers, this volume ranged between 3 and 4 liters above TLC (Loring, 2007), and data from one of them are shown in Fig. 3.

2.4 DATA ANALYSIS

All images were imported into ImageJ (rsbweb.nih.gov/ij/) for further processing. Automatic window and leveling were performed, and the signal intensities were linearly mapped to an eight bit grey or color scale. This look-up table was applied to the whole dataset to better identify areas of intense signal. Typically, the area of the highest intensity was gas in the trachea; thus windowing and leveling were performed with the trachea as the normalizing factor. All data sets were normalized in this fashion, thus avoiding uncertainties in the level of ^3He polarization between runs. Three regions of interest (ROI) were defined: 1) the region containing the airways, 2) the lung parenchyma with high signal intensity (highest 5% of the lookup table), and 3) the remaining lung parenchyma. The sum of the pixel intensities and the areas of each ROI were recorded for each slice. For the two non-airway ROIs, the percentage of the total intensity and volume of each ROI was calculated. An example is shown in Fig. 1.

2.5 STATISTICS

Statistical analysis was performed using Mathworks Matlab software version 7.5.0. An unbalanced 2-Way ANOVA was performed to look for differences in the percent intensity and percent volume ratios between inhalation states and between the high intensity pericardial area ROIs and normal lung parenchyma.

3. Results

Fig. 2 depicts a complete TLC multi-slice dataset from of one of the divers showing a high-intensity pericardial region in multiple slices. Fig. 3 depicts mid-coronal slices from the same diver acquired after three different breathing maneuvers. The top row shows the static ventilation images of the lungs after inhalation of the ^3He gas mixture from FRC. The middle row shows the images of the same subject's lungs after inhaling the gas at TLC and the bottom row shows the same subject's images at TLC+GI. Note that at FRC+IL, the signal intensity is relatively homogenous with a signal-to-noise-ratio (SNR) of 63, whereas at TLC and TLC+GI the pericardial region of the lower left lung is characterized by very high signal intensity with a small amount of high intensity in the lower medial region of the left lung with an SNR of 150. These are areas around the negative curvature of the lung surrounding the heart and dorsal caudal parts of the lungs. The same observations were made in all seven subjects at TLC and in all four divers at TLC+GI.

We characterized the degree of inhomogeneity of specific ventilation at the various target lung volumes as follows. Within the non-airway lung, we computed the respective volumes and summed intensities of ^3He of the high-intensity and remaining regions. From these data we computed two indices of the nature of the high intensity region. First, we assessed the simple volume fraction of that region, relative to the total volume of the non-airway lung. Second, we characterized the mean specific ventilation within each of the two regions by summing the intensities of each voxel. These were expressed as fractions of the total intensity. Pooled data are shown in Table 1.

To evaluate the quantitative significance of the high-intensity region, we reasoned that the ratio of the fractioned intensities to the fractionated volumes would be near 1.0 if specific ventilation

were uniform. We therefore assessed the specific ventilation in the two regions by computing the ratio of summed intensity to summed volume for each region (see Table 1), expressing this relative to the ratio of total intensity to total volume. This is displayed in the plot in Fig. 4, where, for example, most of the lung has a normalized concentration near 1.0, as expected for uniform specific ventilation. By contrast, the high intensity region has a normalized concentration near 2.7 at TLC and 4.3 at TLC+GI, showing a significant departure from homogeneity. An ANOVA revealed statistically significant differences in the fractional ventilation at different lung volumes ($p=0.0032$) and between the normal lung parenchyma and high intensity pericardial regions at TLC and TLC+GI ($p=0.0268$).

There are a variety of other measures of regional heterogeneity, principally based on regional estimates of coefficients of variation (CV), over regions or boxes of interest. Such measures include the simple CV for the whole lung, spatial maps of CV for a fixed box size (Tzeng, 2009), and various techniques of an autocorrelative nature often based on fractal ideas where the box size is systematically varied. The most established of these latter methods is the so-called method of “box-counting” (Bassingthwaite, 1994), popularized by Glenny et al. (1991, 1999). However, these approaches are all based on regional averages, and are inappropriate to our central question: Where does the inspired gas go? The methods we use as outlined above are the most direct and straightforward approach to this.

4. Discussion

The principal findings of this study are threefold. First and most surprisingly and potentially most importantly, in normal subjects at TLC, there was a striking regional heterogeneity in fractional ventilation of the lung, characterized by markedly increased ventilation in the pericardial region compared with the relatively uniform ventilation throughout the rest of the lung. Second, this effect was more pronounced in the divers at lung volumes above TLC. Third, the distribution of fractional ventilation regionally was relatively uniform at FRC+1L, confirming previous observations of a small non-gravitational cephalocaudal gradient of specific ventilation in the supine posture (Hubmayr, 1983).

What mechanisms may account for this striking behavior? It is certainly true that both the overall lung compliance (here and throughout we refer specifically to the tangent compliance) and the local specific compliance of lung regions drop progressively and markedly as TLC is approached. However, even small variations in the specific compliances that exist throughout the lung near TLC can cause large variations in their ratios, and therefore a commensurate variation in the distribution of the inspire.

Why might there be a preferential increase in expansion in the region of the lung near the heart, particularly on the left side? The argument presented above simply assumes the existence of a variable (but low) compliance regionally, and does not address any specific anatomical features that might contribute. In this context, we note that in addition to the lung parenchyma stiffening at high volumes, the strain on the visceral pleural membrane is also increasing, with a corresponding increase in pleural membrane tension. The latter is known to significantly contribute to the work done expanding the lung (Hajji, 1979). An important feature of the tensed pleural membrane is that, in the coupling of its tension with the geometric curvature of the lung, there is a stress jump across the pleura, effectively changing the local recoil pressure seen by the subjacent parenchyma. The concept of a stress jump is equivalent to a difference in recoil pressure viewed from the point of view of the lung as a whole, including the pleura, and the local recoil seen by the lung parenchyma. The costal surface of the lung is convex, and so the effect of this stress jump is to support a portion of transpulmonary pressure, i.e. restraining the parenchyma subjacent to the costal surface of the lung to a lower volume than would pertain if local lung recoil were equal to the difference of alveolar and pleural pressures.

By contrast, the pericardial pleural surfaces (and to a lesser extent, the diaphragmatic pleural surface) display a sharp negative curvature. In these regions, the stress jump promotes expansion of the subjacent parenchyma, and in consequence, such regions can accommodate a disproportionately large fraction of the final inspiratory volume. This idea can also be appreciated through a simple compliance argument, which is essentially equivalent to the idea of a systematic difference in the regional stress jump (and hence local recoil) in the pericardial region. Consider the pressure cost of expanding a region of lung near the rib cage, where the pleura is convex - any expansion of subpleural parenchyma must also be associated with increasing the strain and stress in the pleura locally, and thus the pleura will tend to make such regions stiffer than they otherwise would be. Conversely, in the pericardial region especially, the concave curvature of the pleural surface means that any local expansion of the subjacent parenchyma will be associated with a release of strain and tension in the pleura, thus tending to make these regions less stiff.

These ideas apply whenever there are variations in curvature, especially in its sign. With respect to the negative curvature of the diaphragm, we note that this is preserved even at high lung volumes in isolated lung preparations. It does, however, tend to flatten out slightly (and with a commensurate small increase in local volume relative to the rest of the lung), consistent with a role played by the tensed pleura. On the other hand, as the diaphragmatic surface flattens, its curvature decreases, and even in the face of increased pleural tension, this decrease in curvature mitigates against any substantial stress jump in that region, consistent with what one sees in the isolated lung. Note further that *in vivo*, the presence of the heart does not alter our interpretation of the data. In particular, within the constraints of whatever geometry the configuration of the thorax and heart has assumed, the lung will match that by whatever distortion is necessary, consistent with mechanical equilibrium. This in turn requires differential inflation if local recoil pressures are different, which we argue is a necessary consequence of the sharply increasing pleural tension and the different curvatures (especially the high negative curvature pericardially). With respect to absolute volumes, note that we are not suggesting that the additional GI volume, or even a substantial portion of it, need fill the pericardial region. Rather, our argument rests on preferential filling, such that even if the majority of this last portion of the inspire is uniformly distributed, there is a significant quantity that preferentially fills the pericardial region.

One can make the above argument semi-quantitative. Hajji et al. (1979) found that tension (T) in the pleura of pig and man exceeds 15000 dyne/cm at a lung recoil of 25 cmH₂O, and that this is a very weak lower bound for pleural tension at higher lung volumes, since the increase of tension is extremely sharp with increasing recoil at these levels. If the radius (R) of the heart is taken to be on the order of 5 cm, then the Laplace relation $\Delta P = 2 T/R$ implies a stress jump (equivalently, the change in subjacent lung recoil) of 6000 dyne/cm², or 6 cmH₂O. In other words, there is an additional stress of at least that amount in the pericardial region that necessarily changes the local fractional ventilation to that region. This semiquantitative estimate is thus consistent with the ideas presented above on the underlying mechanisms contributing to our findings. In particular, this argument points to a specific and anatomically based mechanism for the pericardial location of preferential filling of the last portion of an inspire, either near TLC in normal subjects, or at volumes above TLC in elite divers.

Our physiological interpretations given above are further supported by a recent case study of hyperinflation of a diver performing a GI maneuver (Eichinger, 2008). The lung was assessed with traditional proton MRI, where it was qualitatively observed that in the hyperinflated state there was a substernal herniation of the lung, and moreover, the costodiaphragmatic angle was increased. These suggest preferential filling of this region, similar in location to the pericardial regions we found receiving the last portion of the GI inspire.

4.1 Limitations

Several points of limitation need to be acknowledged. First, our sample size is small; this is due to practical reasons of the availability and participation consent of individuals within the elite diving community, itself comprising a very rare population. This precludes addressing questions such as differences between controls and the divers at TLC, and between males and females. On the other hand, the striking findings and significant differences shown in Fig. 4 argue that this is not a serious drawback of the study. Second, there is a qualitative nature to the admittedly artificial separation of intensities in high and moderate regions, and in the drawing of lung boundaries. To this end there is an unavoidable subjective aspect to our work. Nevertheless, the robust results we have found, together with testing variations in threshold intensities, suggest that our physiologic conclusions are only weakly dependent on the assumptions made in the data analysis procedure. Third, magnetic field and radio-frequency (RF) coil inhomogeneities could contribute to differences in MR signal intensities observed in different parts of the lung. However, it should be noted that the RF lung coil was previously tested to have <20% inhomogeneity, which should be adequate for the present study. In addition, the magnetic field was shimmed on each subject on the water proton signal, prior to acquiring the ^3He lung image, so that magnetic field inhomogeneities should be negligible. Indeed, this is supported by the observation that there was little heterogeneity observed from inhalations at FRC, consistent with homogeneous ventilation in normal control subjects at modest lung volumes (Fig. 3), and ruling out any significant apparent heterogeneities associated with field inhomogeneities.

4.2 Conclusions

We used hyperpolarized ^3He MRI to show previously unreported regional ventilation differences at large lung volumes. We found that a disproportionately large fraction of the inspired gas goes to the pericardial region of the lower left lung. At high lung volumes, these observations are consistent with the effect of high pleural tension in the concave pericardial region, which leads to a reduction in local recoil. Compared to the rest of the lung, the local specific compliance is higher, leading to higher specific ventilation.

5. Acknowledgments

We thank Xiangzhi Zhou, Joey Mansour, and Haihua Bao for technical help. Supported by NIH grant R33-EB001689 and NASA grant NAG9-1469.

6. References

- Altes TA, Rehm PK, Harrell F, Salerno M, Daniel TM, De Lange EE. Ventilation imaging of the lung: comparison of hyperpolarized helium-3 MR imaging with Xe-133 scintigraphy. *Acad Radiol* 2004;11:729–734. [PubMed: 15217589]
- Bassingthwaighe, JB.; Liebovitch, LS.; West, BJ. *Fractal Physiology*. Oxford University Press; Oxford: 1994.
- Brenner DJ, Hall EJ. Computed tomography--an increasing source of radiation exposure. *N Engl J Med* 2007;357:2277–2284. [PubMed: 18046031]
- Dail CW. "Glossopharyngeal breathing" by paralyzed patients; a preliminary report. *Calif Med* 1951;75:217–218. [PubMed: 14870041]
- Eichinger M, Waltersbacher S, Scholz T, Tetzlaff K, Röcker K, Muth CM, Puderbach M, Kauczor HU, Sorichter S. Lung hyperinflation: foe or friend? *Eur Respir J* 2008;32:1113–6. [PubMed: 18827157]
- Engel, L. Dynamic distribution of gas flow. In: Fishman, A.; Macklem, P.; Mead, J., editors. *Handbook of physiology; The Respiratory System*. American Physiological Society; Bethesda, Maryland: 1986. p. 575-593.
- Glazier JB, Hughes JM, Maloney JE, West JB. Vertical gradient of alveolar size in lungs of dogs frozen intact. *J Appl Physiol* 1967;23:694–705. [PubMed: 4862981]

- Glenny RW, Lamm WJ, Albert RK, Robertson HT. Gravity is a minor determinant of pulmonary blood flow distribution. *J. Appl. Physiol* 1991;71:620–629. [PubMed: 1938736]
- Glenny, RW. Heterogeneity in the Lung: Concepts and Measurement. In: Hlastala, MP.; Robertson, HT., editors. *Complexities in Structure and Function of the Lung*. Marcel Dekker; New York: 1999. p. 571-609.chap. 11
- Hajji MA, Wilson TA, Lai-Fook SJ. Improved measurements of shear modulus and pleural membrane tension of the lung. *J Appl Physiol* 1979;47:175–181. [PubMed: 468657]
- Happer W, Miron E, Schaefer S, Schreiber D, van Wijngaarden WA, Zeng X. Polarization of the nuclear spins of noble-gas atoms by spin exchange with optically pumped alkali-metal atoms. *Phys. Rev. A* 1984;29:3092–110.
- Hubmayr RD, Walters BJ, Chevalier PA, Rodarte JR, Olson LE. Topographical distribution of regional lung volume in anesthetized dogs. *J Appl Physiol* 1983;54:1048–1056. [PubMed: 6853280]
- Lindholm P, Nyren S. Studies on inspiratory and expiratory glossopharyngeal breathing in breath-hold divers employing magnetic resonance imaging and spirometry. *Eur J Appl Physiol* 2005;94:646–651. [PubMed: 15942772]
- Lindholm P, Norris CM, Braver JM, Jacobson F, Ferrigno M. A fluoroscopic and laryngoscopic study of glossopharyngeal insufflation and exsufflation. *Respir. Physiol. Neurobiol.* 2009in press
- Loring SH, O'Donnell CR, Butler JP, Lindholm P, Jacobson F, Ferrigno M. Transpulmonary pressures and lung mechanics with glossopharyngeal insufflation and exsufflation beyond normal lung volumes in competitive breath-hold divers. *J Appl Physiol* 2007;102:841–846. [PubMed: 17110514]
- Milic-Emili, J. Static distribution of lung volumes. In: Fishman, A.; Macklem, P.; Mead, J., editors. *Handbook of physiology; The Respiratory System*. American Physiological Society; Bethesda, Maryland: 1986. p. 561-574.
- Milic-Emili J, Henderson JA, Dolovich MB, Trop D, Kaneko K. Regional distribution of inspired gas in the lung. *J Appl Physiol* 1966;21:749–759. [PubMed: 5912744]
- Nygren-Bonnier M, Wahman K, Lindholm P, Markstrom A, Westgren N, Klefbeck B. Glossopharyngeal pistoning for lung insufflation in patients with cervical spinal cord injury. *Spinal Cord*. 2008published online nov 11
- Secombe LM, Rogers PG, Mai N, Wong CK, Kritharides L, Jenkins CR. Features of glossopharyngeal breathing in breath-hold divers. *J Appl Physiol* 2006;101:799–801. [PubMed: 16690794]
- Tzeng YS, Lutchen K, Albert M. The difference in ventilation heterogeneity between asthmatic and healthy subjects quantified using hyperpolarized ³He MRI. *J Appl Physiol* 2009;106:813–22. [PubMed: 19023025]

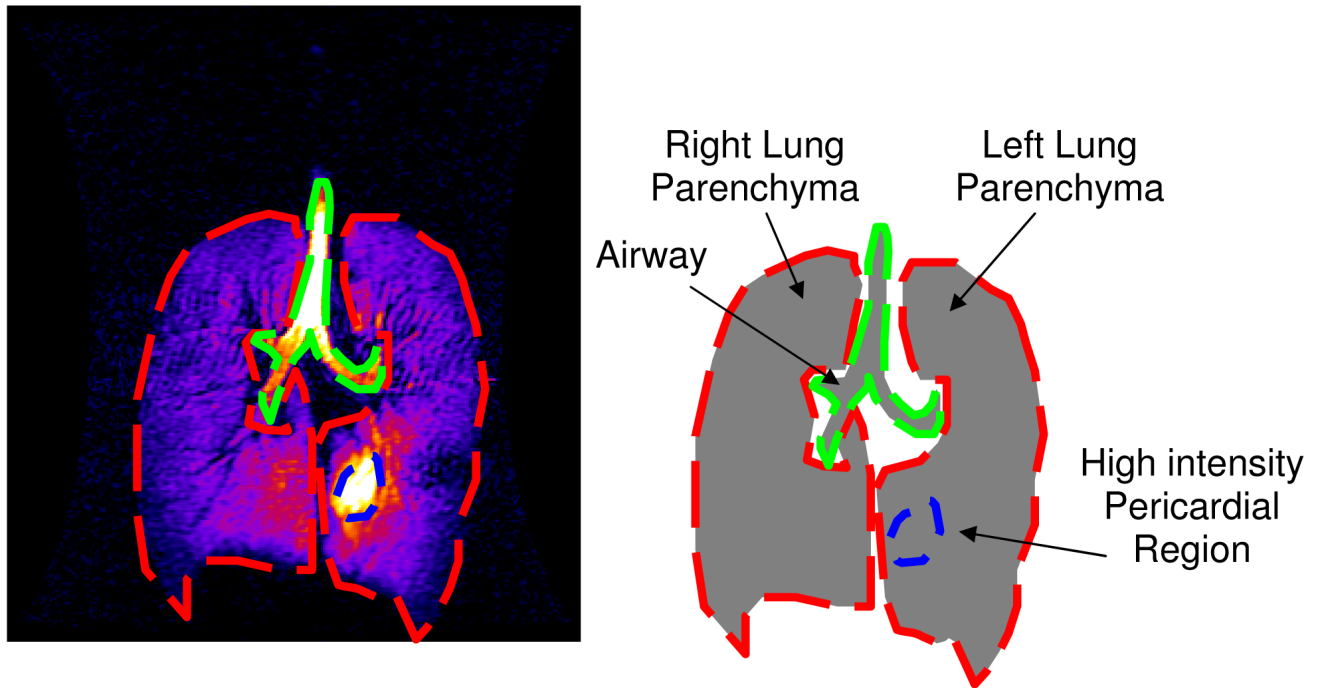


Fig. 1. This figure depicts the image segmentation for data presented in Table 1. The airways were excluded manually, and the region(s) of parenchyma enclosed by colored dashes were identified by a threshold intensity. The volume and signal intensity was measured in the high intensity regions and the rest of the lungs.

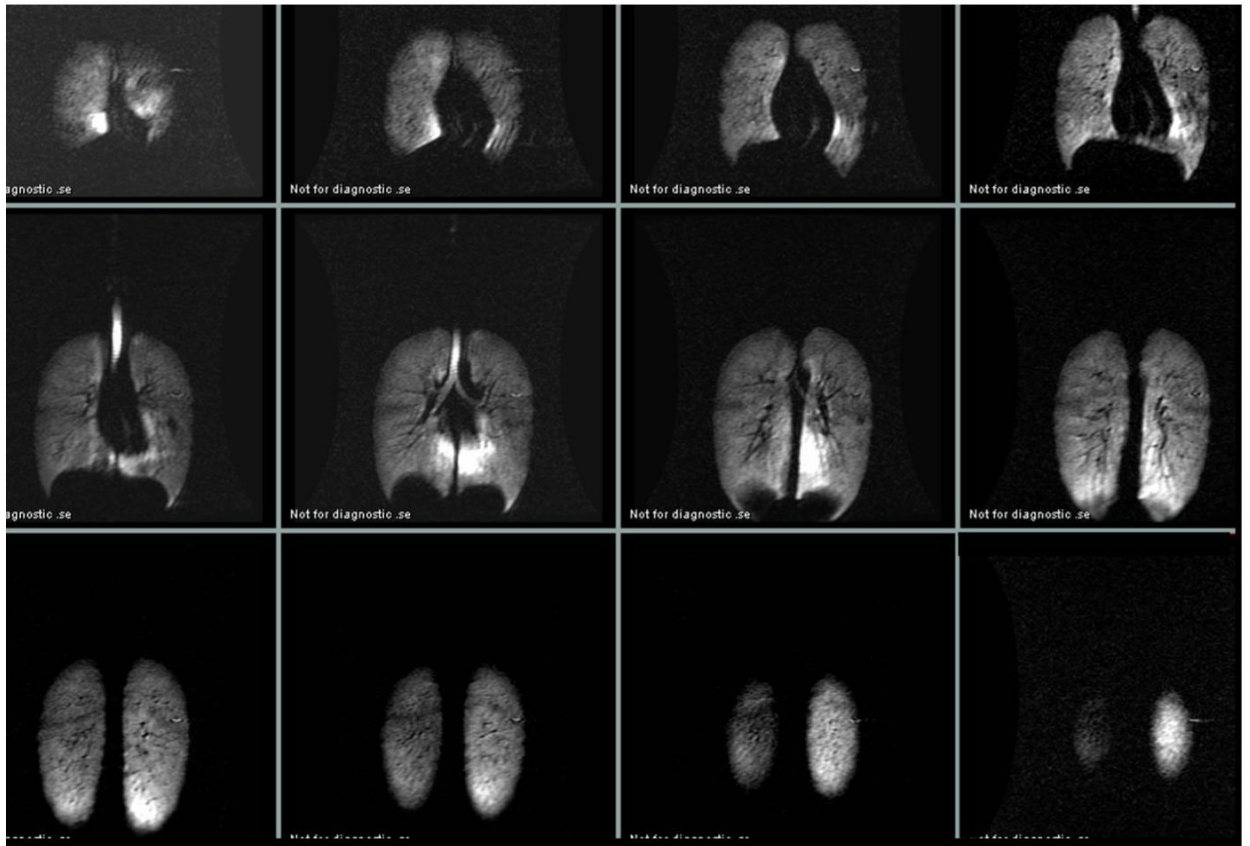


Fig. 2. Signal intensity at total lung capacity in one subject. After inhalation to total lung capacity the subject exhaled 1 liter of air and thereafter inhaled a liter of hyperpolarized ^3He prior to holding his breath during scanning.

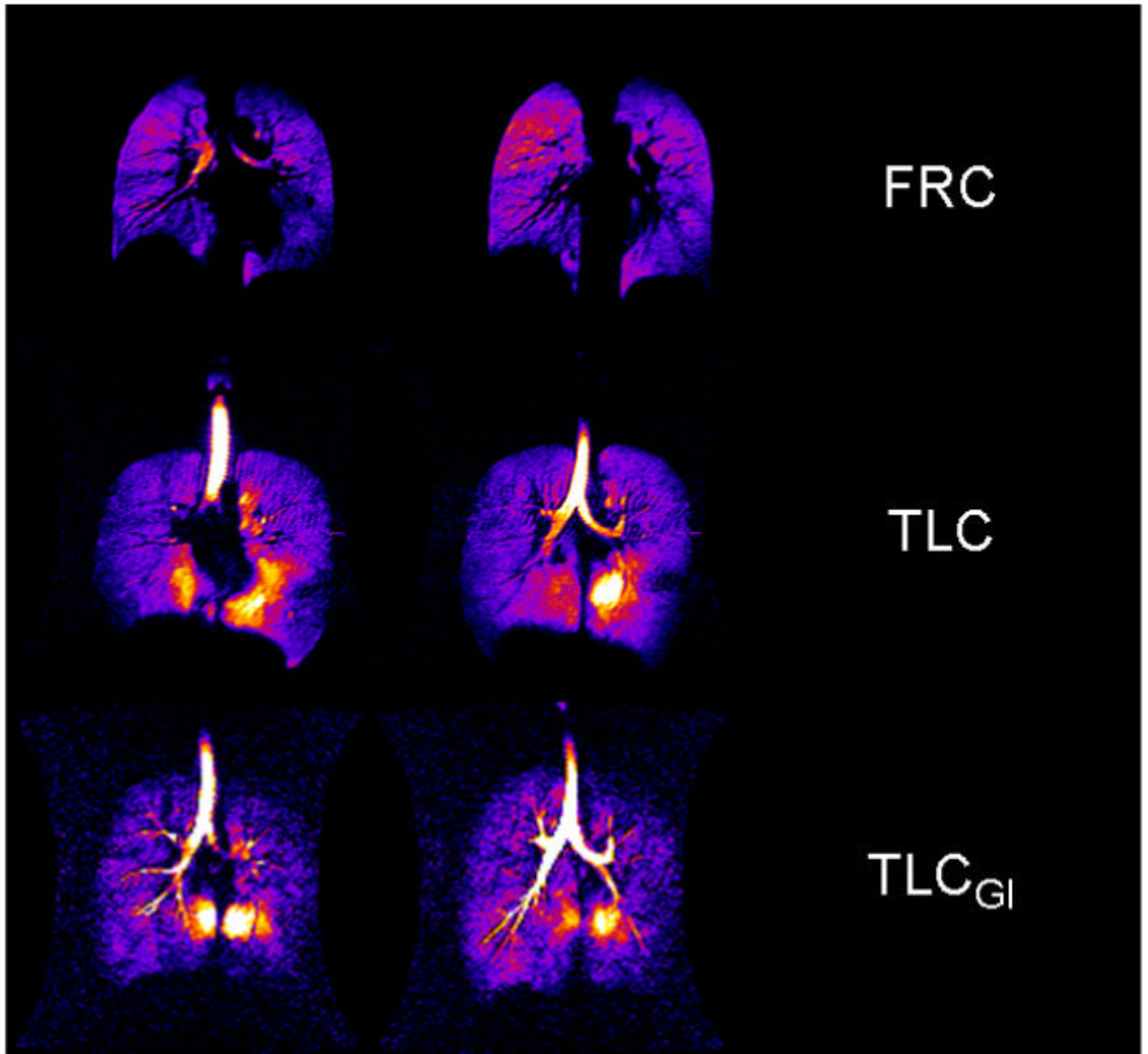


Fig. 3. Fractional ventilation (dilution ratio) in two coronal slices (mid thoracic) at FRC+1L, TLC, and TLC+GI. The final liter of inhaled or insufflated gas was drawn from a reservoir of hyperpolarized ^3He .

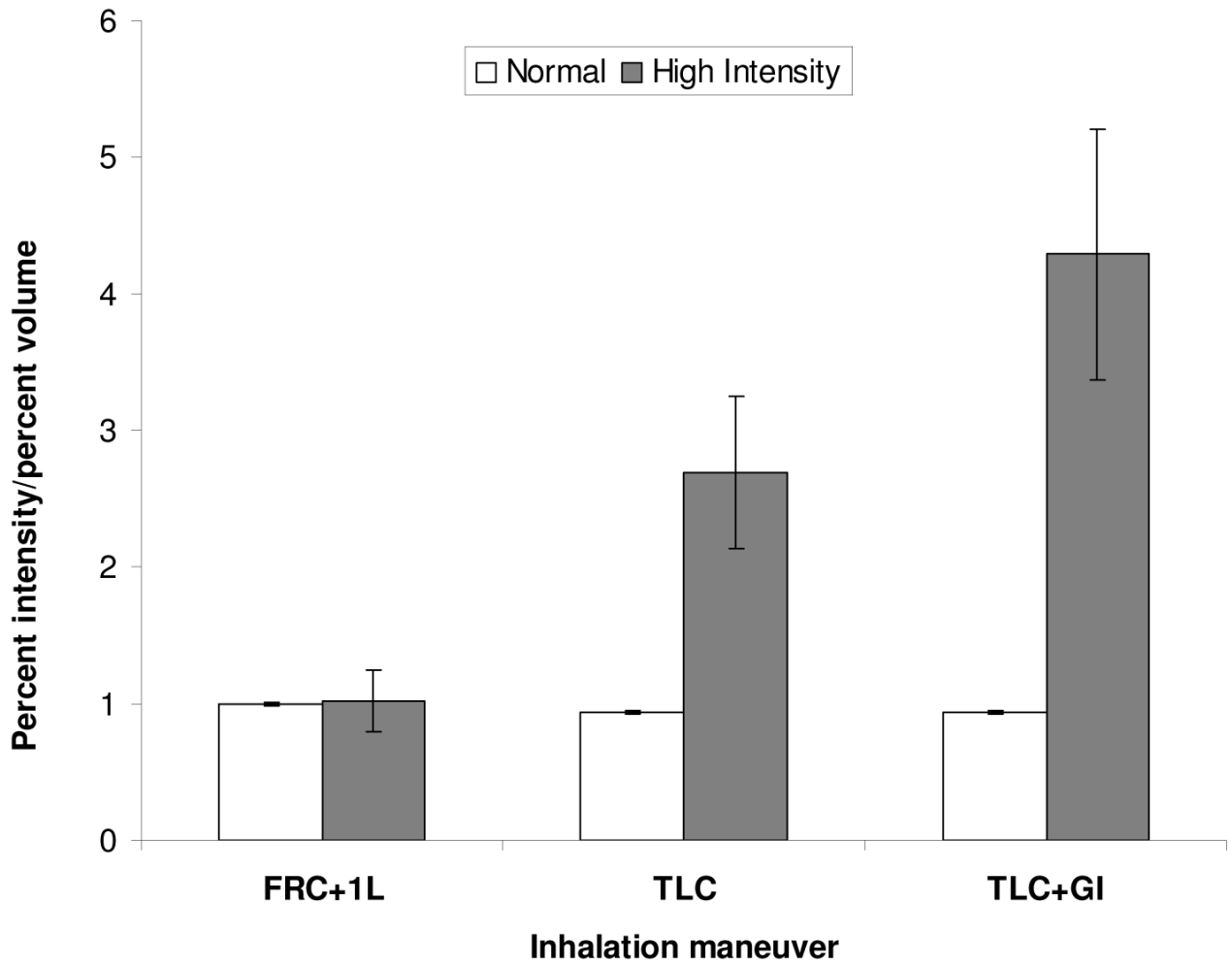


Fig. 4. Plot of the average ratio of volume fraction and intensity fraction at each inhalation volume. There is marked increase in this ratio in TLC and in TLC+GI in the pericardial region of high intensity.

Table 1
Pooled data for volume fraction, intensity fraction, and fractional ventilation

Lung Volume	n	Region	Volume fraction (VF)	Intensity fraction (IF)	Fractional ventilation (IF/VF)
FRC+IL	5	low intensity	96.31±1.22	96.01±2.12	1.00±0.01
		high intensity	3.69±1.2	3.99±2.12	1.02±0.22
TLC	7	low intensity	96.39±1.80	91.04±2.93	0.94±0.01
		high intensity	3.61±1.80	8.96±2.93	2.69±0.56
TLC+GI	4	low intensity	98.03±0.33	91.86±0.46	0.94±0.01
		high intensity	1.97±0.33	8.14±0.46	4.29±0.92